

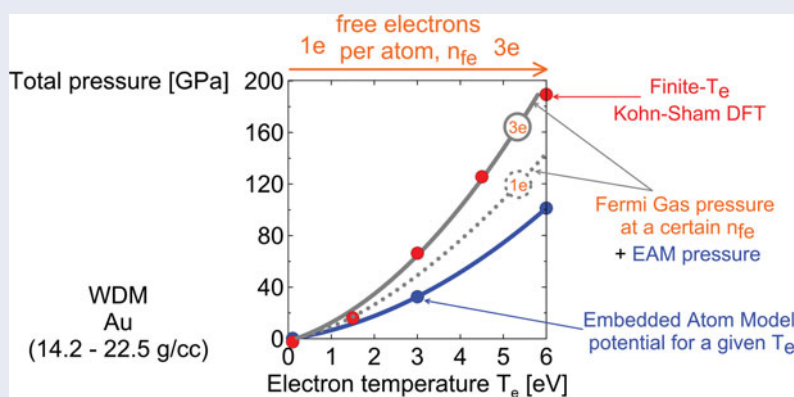
Warm dense gold: effective ion–ion interaction and ionisation

V. V. Stegailov ^{a,b,c} and P. A. Zhilyaev^{a,b}

^aDepartment of Atomistic Modelling and Theory of Condensed Matter and Non-ideal Plasma, Joint Institute for High Temperatures, Russian Academy of Sciences, Moscow, Russia; ^bDepartment of Molecular and Chemical Physics, Moscow Institute of Physics and Technology, Dolgoprudny, Russia; ^cMoscow Institute of Electronics and Mathematics, National Research University Higher School of Economics, Moscow, Russia

ABSTRACT

Warm dense matter is a peculiar state with solid densities and temperatures 1 – 100 eV. Its *ab initio* description waits united efforts of quantum chemistry, condensed matter and plasma physics. We use the finite temperature Kohn–Sham density functional theory (a ‘workhorse’ in this field) to study the pressure build-up with increase of electronic temperature in crystal and amorphous warm dense matter (WDM) gold. We compare the *ab initio* results with the effective ion–ion interaction model and reveal the possibility to separate the free electron contribution to the total pressure in WDM and to determine the corresponding degree of ionisation. For the sake of clarity, we try to describe our findings using the proper framework of statistical physics and briefly review the free energy models for WDM.



ARTICLE HISTORY

Received 6 May 2015
Accepted 2 October 2015

KEYWORDS

Density functional theory;
excited states; free electrons

1. Introduction

Building a rigorous theory for molecules in excited states is one of the major challenges for quantum chemistry [1]. Nowadays, the corresponding methods developed for isolated systems pave the way towards applications in condensed matter studies [2–4]. Plasma and warm dense matter (WDM) studies are the next field that, in principle, could benefit from the application of chemical accuracy techniques. However, in this case one has to treat not only periodic systems but also systems at essentially non-zero temperatures. This is a very ambitious effort that has been commenced recently.

Quantum mechanical description of electrons in condensed phase is a general problem of the highest importance. However, the rigorous wave-functions-based theory is very complicated even for ground state

($T_e = 0$), the finite temperature (FT) case being much farther from applicability in practice. Only recently accurate quantum Monte Carlo approaches have been developed in this field [5]. That is why the Kohn–Sham density functional theory (KS DFT) method in the FT formulation became a tool of choice (for some first examples of its applications for plasma and warm dense metals see e.g. see [6–8]). Orbital-free DFT is a very promising approach with respect to computational efficiency (e.g. [9–11]).

Temperature implies the necessity of the statistical description of the coupled system of electrons and ions. Statistical physics deploys the free energy \mathcal{F} as a starting point for the theory. At the atomistic level, one needs to describe the ion dynamics and therefore to know how to calculate forces acting on them. Moreover, in experiments with plasma or WDM, electrons and ions frequently are not in thermodynamic equilibrium. These needs

(statistical and atomistic description including non-equilibrium phenomena) determine the complexity of building a proper theory.

In our previous work [12], we have presented the results that raised questions about how we should bridge the FT KS DFT description with classical atomistic scale. In this work, we present new results for WDM gold that emphasise the need for rethinking the common concepts used in modelling and simulation of WDM at the *ab initio* level.

The structure of the paper is as follows. In Sections 2 and 3, we review the free energy models that are deployed in *ab initio* theory of WDM in equilibrium and non-equilibrium cases. In Section 4, we present the details of the FT KS DFT calculations performed in this work. Sections 5 and 6 provide our novel results on the analysis of the interatomic forces and pressure in WDM gold. In Section 7, we give the conclusions.

2. Free energy and equation of state

An equation of state (EOS) is a relation of density, temperature and pressure in the system. These data are required for numerous applications and the EOS models have a long history of development [13]. Generally speaking, the aim is to develop EOS models for the coupled system of electrons and ions at different temperatures and densities. At the moment, there are well-established models for selected cases only. The number of difficulties in such studies is immense.

Among other major problems, we can point out the question of the separation of electrons into bound and free (or localised and delocalised) that is a general problem for non-ideal plasma physics (e.g. [14–17]) including EOS models (e.g. [18]), ion–ion correlations [19,20], continuum lowering [21] and plasma–plasma phase transition [22], for models of laser–matter interactions (see below), models of swift ion tracks (e.g. [23–25]) and other high energy density physics applications.

In the so-called chemical model of plasma (which represents plasma as a mixture of interacting electrons, ions, atoms and molecules), the Helmholtz free energy is taken as a sum of the ideal contributions of atoms, ions, molecules and non-degenerate electrons (the term ‘ideal’ means non-interacting) plus the free energy contribution due to inter-particle interactions [26]. In dense systems with degenerate electrons, there is another situation.

The realm of material science problems is restricted to the moderate temperatures $T \ll T_F$, where T_F is the Fermi temperature. In this case, we can neglect temperature effects in the electron subsystem (especially when there is a non-zero bandgap). The mass difference between electrons and ‘heavy’ particles (atoms, ions) justifies

the adiabatic Born–Oppenheimer approximation (BOA). In the BOA framework, the ionic ‘Hamiltonian’ is (e.g. [27])

$$H(\{\mathbf{P}_i, \mathbf{R}_i\}) = \sum_{i=1}^N \frac{\mathbf{P}_i^2}{2M} + \frac{1}{2} \sum_{i \neq j} \frac{Z^2 e^2}{|\mathbf{R}_i - \mathbf{R}_j|} + E(\{\mathbf{R}_i\}), \quad (1)$$

where $\{\mathbf{P}_i\}$ and $\{\mathbf{R}_i\}$ are the set of momentum and coordinate operators of ions and $E(\{\mathbf{R}_i\})$ is the electronic energy which depends parametrically on nuclear positions (for simplicity of notation we assume the system of N atoms of the same type with the density $\rho = N/V$). The thermodynamics of the system is derived from the knowledge of the Helmholtz free energy

$$\mathcal{F}(\rho, T) = -k_B T \log \left[\text{Tr} \left(\exp \left(-\frac{H(\{\mathbf{P}_i, \mathbf{R}_i\})}{k_B T} \right) \right) \right]. \quad (2)$$

The term $E(\{\mathbf{R}_i\})$ can be computed at various levels of approximation, e.g. using KS DFT.

In the BOA framework, one can deploy effective interionic (interatomic) potentials that being mainly empirical reproduce accurately enough the potential energy surface $E(\{\mathbf{R}_i\})$. Using such effective potentials, one can calculate from atomistic models the free energy \mathcal{F} , the EOS and other thermodynamic properties of particular systems (e.g. see [28,29]). Having eliminated the need to describe explicitly the electronic component, one can even go beyond pure hydrogen [27] in the treatment of nuclear quantum effects (e.g. see [30]).

In the case of lattice dynamics, the quasiharmonic approximation simplifies Equation (2) as (e.g. see [31])

$$\mathcal{F}(\rho, T) = \mathcal{F}_i^{ph}(\rho, T) + E_i(\rho), \quad (3)$$

where \mathcal{F}_i^{ph} is a free energy of phonon subsystem in the harmonic approximation for the given crystal lattice and $E_i(\rho)$ is the binding energy for this lattice (the so-called ‘cold curve’).

There are cases when the proper description of lattice dynamics of metals even at $T \ll T_F$ requires going beyond BOA in an attempt to take the non-adiabatic terms into account (e.g. see the discussion of non-adiabatic effects in phonon spectra of metals [32,33] and the peculiar case of graphene [34]). However, it is not possible to go beyond BOA keeping the same rigour and level of consistency as we have in Equations (2) and (3).

The practical way for going beyond BOA for the description of high temperature states is to add to Equation (3) the thermal contribution of free electrons \mathcal{F}_{fe}

(e.g. [35])

$$\mathcal{F}(\rho, T) = \mathcal{F}_i^{ph}(\rho, T) + E_i(\rho) + \mathcal{F}_{fe}(n_{fe}, T). \quad (4)$$

The difficulty connected with \mathcal{F}_{fe} calculations stems from the fact that for this purpose, one needs the number density of free electrons n_{fe} (i.e. the degree of ionisation). The deployment of the FT Thomas–Fermi model is one way to overcome this problem [35]. Here again, we encounter the question of bound and free electron states separation.

The other practical way of extending Equation (2) or Equation (3) to high temperatures is to change in Equation (1) the ground-state total energy at the fixed position of ions $E(\{\mathbf{R}_i\})$ for the corresponding free energy of electron subsystem $\mathcal{F}_e(\{\mathbf{R}_i\}; T_e)$ at the certain electron temperature:

$$H^*(\{\mathbf{P}_i, \mathbf{R}_i\}; T_e) = \sum_{i=1}^N \frac{\mathbf{P}_i^2}{2M} + \frac{1}{2} \sum_{i \neq j} \frac{Z^2 e^2}{|\mathbf{R}_i - \mathbf{R}_j|} + \mathcal{F}_e(\{\mathbf{R}_i\}; T_e), \quad (5)$$

$$\mathcal{F}(\rho, T) = -k_B T \log \left[\text{Tr} \left(\exp \left(-\frac{H^*(\{\mathbf{P}_i, \mathbf{R}_i\}; T)}{k_B T} \right) \right) \right]. \quad (6)$$

It can be done using the Mermin formulation of FT KS DFT [36]. This ‘free energy Born–Oppenheimer approximation’ has a certain rigorous justification [37]. It is the free energy BOA that is implied in the FT KS DFT molecular dynamics calculations that proved to be very successful in EOS calculation for extreme conditions (see e.g. the examples of quantum molecular dynamics calculations for water [38] and xenon [39]).

3. Two-temperature warm dense matter

Irradiation of solids with ultrashort laser pulses opened an exciting field of research (e.g. [40,41]). New emerging physics is connected with formation of WDM at the initial transient state of material evolution after energy deposition into electron subsystem. WDM is important not only for laser–matter interaction physics but in a wider context as well [42]. WDM in such ultrafast phenomena is a non-equilibrium state that makes it very challenging for theory, modelling and simulation. Usually, WDM can be described as a two-temperature (2T) system when electron and ion subsystems can be considered in quasi-equilibrium at $T_e > T_i$ [43].

Physics of WDM is not a subject of pure fundamental interest. One of the major phenomena where WDM

properties are crucially important in modelling and simulation is laser ablation [44]. Laser ablation is a multiscale phenomenon. Subpicosecond laser excitation transforms material under normal conditions into 2T-WDM in the isochoric way. Relaxation takes about tens of picoseconds before T_i and T_e become equal. This relaxation stage governs the details of ablation mechanism and is the focus of the on-going modelling effort. It can be described at the continuum level (e.g. [45–48]). However, atomistic modelling gives the possibility to capture a richer spectrum of structural transitions and nucleation effects (e.g. [49–59]).

Both in continuum and in atomistic models, it is assumed that the quasi-equilibrium 2T-WDM can be described using thermodynamic concepts. The free energy in this case is treated as a function of two temperatures $\mathcal{F}(\rho, T_i, T_e)$. This is a very questionable approach indeed. But ‘something is better than nothing’ and it is used with a certain success [45–48]. We suppose that the only way forward is to clarify step-by-step the validity of the underlying assumptions and to replace emerging deficiencies with better alternatives.

The usual form of the Helmholtz free energy assumed in the 2T-WDM models mimics the quasiharmonic approximation, that is:

$$\mathcal{F}(\rho, T_i, T_e) = \mathcal{F}_i^{ph}(\rho, T_i) + E_i(\rho) + \mathcal{F}_{fe}(n_{fe}, T_e), \quad (7)$$

The practical use of this ansatz consists of the corresponding expression for the total pressure of 2T-WDM

$$P(\rho, T_i, T_e) = P_i^{th}(\rho, T_i) + P_i(\rho) + P_{fe}(n_{fe}, T_e). \quad (8)$$

The first term is the thermal ion pressure (usually taken as $\rho k_B T_i$), the second term is the so called ‘cold’ pressure and the third term is the electron Fermi gas (FG) pressure. Equation (8) is used in the atomistic models 2T WDM for studies of ablation [49,50,55–57]).

Such atomistic models have several drawbacks:

- it is not clear how to estimate the ionisation degree n_{fe} ,
- there is no consensus on how one should include the electron pressure P_{fe} into ionic equations of motion (some authors use the so-called ‘blast force’ [45,50,58,60]),
- the ‘cold’ pressure P_i is calculated using $T_e = 0$ interionic potentials, but the effective ion–ion interaction essentially depends on T_e .

These drawbacks stem from the *ad hoc* approximate nature of Equation (8). It has been illustrated in [52] and analysed more carefully [12] for fcc WDM aluminum and gold using FT KS DFT calculations. In this work,

we present new results for gold in crystal and amorphous WDM states.

4. Finite temperature Kohn–Sham DFT model

In the FT KS DFT framework, the free energy of electron subsystem in the external potential of ions is given as

$$\mathcal{F}_e^{KS}(\{\mathbf{R}_i\}; T_e) = E_k + E_H + E_{xc} + E_{ei} - T_e S_e, \quad (9)$$

where E_k is the kinetic energy term, E_H is the Hartree term, E_{xc} is the exchange–correlation term, E_{ei} is the electron–ion interaction term and S_e is the entropy of the non-interacting electrons. We do not include in Equation (9) the ion–ion Coloumb interaction $E_{ii} = \frac{1}{2} \sum_{i \neq j} \frac{Z^2 e^2}{|\mathbf{R}_i - \mathbf{R}_j|}$. KS electronic states are populated according to the Fermi–Dirac distribution $f(\epsilon_i) = (e^{(\epsilon_i - \mu)/(k_B T_e)} + 1)^{-1}$, where ϵ_i is the energy of the i th KS state, μ is the chemical potential, k_B is the Boltzmann constant.

In this work, we perform FT KS DFT calculations in the plane-wave basis using VASP [61–64]. The electron–ion interaction for Au is described by the projected-augmented wave (PAW) potential [65,66]. The local density approximation (LDA) approximation is used for E_{xc} [67].

As we reported in our previous paper [12], the major contribution to the pressure build-up comes from the pressure component that corresponds to the kinetic part of the electron density functional and not from its exchange–correlation part. That is why another choice of an exchange–correlation functional (i.e. a GGA one) instead of the LDA approximation should not significantly influence the results.

For calculations of fcc WDM gold properties, we use the PAW model with 11 electrons, the plane-wave basis energy cut-off 230 eV, the energy convergence threshold 10^{-8} and the \mathbf{k} -mesh of $41 \times 41 \times 41$. We have checked that this \mathbf{k} -mesh is dense enough with respect to the pressure convergence (the pressure difference with the $39 \times 39 \times 39$ mesh is only 0.01 GPa). Three densities are considered 16.81, 19.69 and 22.58 g/cc.

For calculations of amorphous WDM gold, we used 32 atoms in the supercell, the same PAW model and basis energy cutoff, the energy convergence threshold 10^{-5} and the \mathbf{k} -mesh of $5 \times 5 \times 5$. We have checked that this \mathbf{k} -mesh is dense enough with respect to the pressure convergence (the pressure difference with the $3 \times 3 \times 3$ mesh is 0.1 GPa). Three densities are considered 19.19, 16.45 and 14.21 g/cc (the corresponding lattice constants are 4.085, 4.300 and 4.515 Å).

5. Effective interionic forces

Among the unusual properties of 2T-WDM is the change in lattice stability of some solids at high levels of electronic subsystem excitation [68]. The bond-hardening effect for gold was initially predicted by FT KS DFT calculations in [68] and got the experimental support in [69]. This effect is not pronounced in simple metals like Al, but is quite high in d -metals like Au. It stems from the renormalisation of the electronic structure at $T_e \sim T_F$ and results in the dependence of the interatomic interaction in 2T-WDM material on electronic temperature T_e (and not only for metals [68,70,71]). Therefore T_e changes — effectively — mechanical, thermodynamic and other properties of a solid, i.e. its EOS.

The bond hardening in fcc Au manifests itself by the increase of the phonon frequencies and the increase of pressure [52,68]. These facts illustrate certain aspects of the changes with T_e that experience the potential energy surface governing ion dynamics of warm dense metal. However, because of the lattice symmetry, we have no information about the effects of T_e on the ionic forces (they always vanish in a perfect crystal lattice). That is why here we consider the forces in 2T-WDM amorphous metals. These forces are the Hellmann–Feynman forces acting on ions:

$$\mathbf{F}_i^{KS} = - \frac{\partial \mathcal{F}_e^{KS}(\{\mathbf{R}_i\}; T_e)}{\partial \mathbf{R}_i}. \quad (10)$$

These forces are the direct consequence of the free energy BOA ‘Hamiltonian’ Equation (5) and are known to be consistent with the FT KS DFT [72]. They are used in very prolific quantum molecular dynamics applications (e.g. [38,39]). At the same time, it should be emphasised that these forces have only some averaged meaning with respect to electronic non-adiabatic transitions [73]. Recently, an implementation of the Ehrenfest-like dynamics in the tight-binding framework for WDM modelling and simulation has appeared [74,75] that describes such electronic non-adiabatic transitions and their effects on atomic forces explicitly.

In [76], the dependence of the interatomic potential for tungsten on T_e was considered. In [51–53], the electronic-temperature-dependent (ETD) interatomic potential for gold in the framework of the embedded atom method (EAM) [77] was developed as well as a numerical scheme that incorporated this ETD-potential into atomistic modelling techniques using LAMMPS [78,79]. Later, this ETD EAM model was successfully used in the study of structural dynamics of laser-irradiated gold nanofilms [54]. Recently, effective ion–ion pair potentials for Al, Na and

K for densities and temperatures relevant to the WDM regime have been developed [80].

The ETD EAM model $E_{ii}^{\text{EAM}}(\{\mathbf{R}_i\})$ for gold [51–53] was built by the force matching (FM) method using the data set of *ab initio* forces and energies obtained from FT KS DFT for a big set of atomic configurations $[\{\mathbf{R}_i\}_1, \{\mathbf{R}_i\}_2 \dots]_{\text{FM}}$. The FM procedure was performed for three values of T_e (0.1, 3 and 6 eV). In this work, in order to show the accuracy of the ETD EAM model, we illustrate the comparison of per atom forces in the ETD EAM model

$$\mathbf{F}_i^{\text{EAM}} = -\frac{\partial E_{ii}^{\text{EAM}}(\{\mathbf{R}_i\})}{\partial \mathbf{R}_i} \quad (11)$$

and FT KS DFT forces (Equation (10)) for the same atomic configurations of amorphous WDM gold.

We obtain three test configurations $[\{\mathbf{R}_i\}_{0.1 \text{ eV}}; \{\mathbf{R}_i\}_{3 \text{ eV}}; \{\mathbf{R}_i\}_{6 \text{ eV}}]_{\text{test}}$ by equilibration at $T_i = 3000$ K of the amorphous structures of 32 atoms in the cubic simulation box with periodic boundary conditions using ETD EAM models for $T_e = 0.01, 3$ and 6 eV, respectively. Then for each of these test configurations, the FT KS DFT calculations are performed. The comparisons of the projections of per atoms forces ($F_{i,x}, F_{i,y}, F_{i,z}$) are shown on Figure 1. These comparisons show a good accuracy of approximation of the $\mathcal{F}_e^{\text{KS}}(\{\mathbf{R}_i\}; T_e)$ free energy surfaces by the EAM potential models at $T_e = 0.1, 3$ and 6 eV. Here, it is important to note that the ‘FM’ and ‘test’ sets of configurations are independent.

6. Total pressure and its free electron part

The bond hardening manifests itself as a significant pressure build-up in the electronically excited metal. In [52], the comparison of the pressure in *ab initio* calculations based on FT KS DFT p^{KS} with the pressure build-up in the ETD EAM potential model (based on the same *ab initio* results) p^{EAM} allowed to propose an *ad hoc* separation of the pressure increase due to localised and due to delocalised electrons in 2T-WDM gold. In the atomistic model for ablation of gold [51–53], the pressure build-up due to localised electrons was taken into account by the ETD EAM potential that effectively describes the dependence of the binding pressure on electron excitation $P_i = P_i(\rho; T_e)$. In [52,53] — additionally — the pressure build-up due to delocalised electrons in 2T-WDM gold was taken into account using the blast force fitted to match the difference ($p^{\text{KS}} - p^{\text{EAM}}$).

Despite its fundamental significance, the calculation of pressure in the general context of atomistic modelling and simulation is a subject of on-going research (e.g. [81,82]). In this work, we are making an attempt to analyse the

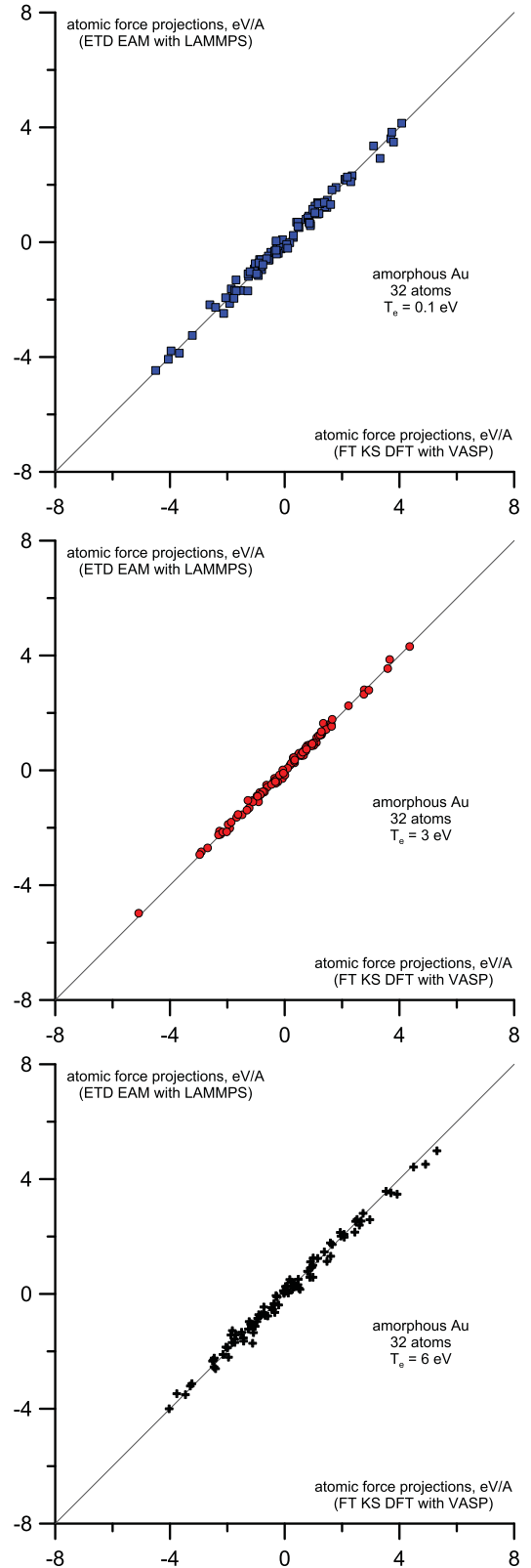


Figure 1. The projections of per atoms forces ($F_{i,x}, F_{i,y}, F_{i,z}$) of the *ab initio* density functional theory model calculation (FT KS DFT) and the empirical classical interionic potential calculation (ETD EAM) for the test configurations. For each configuration the corresponding electronic temperature T_e is used in FT KS DFT calculation and the corresponding EAM potential is used. VASP and LAMMPS codes are used for DFT and EAM model calculations respectively.

electronic contribution to the total pressure in 2T-WDM metals and to clarify the representation Equation (8).

In the case of a classical atomistic model with the ETD EAM potential, pressure can be determined as

$$P^{\text{EAM}} = \rho k_B T_i - \left\langle \frac{\partial E_{ii}^{\text{EAM}}}{\partial V} \right\rangle. \quad (12)$$

In the *ab initio* case, if we limit our consideration to the case of lattice dynamics we see the following sequence of approximations on the way from a ground state model to a 2T WDM model: Equation (3) \rightarrow Equation (4) \rightarrow Equation (7) \rightarrow Equation (8).

If we are interested in a general consideration, then we can obviously generalise Equation (6) to the 2T case with $T_i \neq T_e$. Then, we can assume that the atomistic models built with the corresponding ‘Hamiltonian’ Equation (5) will give us reasonable results if statistical averaging is performed (for example, along a quantum molecular dynamics trajectory, e.g. see [38,39]). In the case of quantum molecular dynamics based on FT KS DFT, the total pressure is conventionally calculated as

$$P^{\text{KS}} = \rho k_B T_i - \left\langle \frac{\partial (E_{ii} + \mathcal{F}_e^{\text{KS}})}{\partial V} \right\rangle. \quad (13)$$

Here, for the sake of simplicity we will assume in the following that

- $T_i = 0$ and the first term (the thermal ion pressure component) vanishes,
- we can neglect the fluctuations of the ‘instantaneous pressure’ $-\frac{\partial E_{ii}^{\text{EAM}}}{\partial V}$ and $-\frac{\partial (E_{ii} + \mathcal{F}_e^{\text{KS}})}{\partial V}$ in different configurations $\{\mathbf{R}_i\}$ (in the appropriate ensemble, NVE or NVT).

These assumptions bring us to the typical pressure values of P^{EAM} and P^{KS} that are obtained in static *ab initio* atomistic calculations.

Figure 2 shows the comparison of P^{KS} and P^{EAM} obtained for fcc WDM gold at different densities. The significant difference ($P^{\text{KS}} - P^{\text{EAM}}$) [12,52] suggests that the delocalised component of electron subsystem does not contribute to the ionic forces and the pressure P^{EAM} corresponds only to the binding component of the electron subsystem determined by localised electrons.

Conduction band electrons in metals are usually considered to be close to the FG model. The FG model is a simple quantum theory that has one input parameter n_{fe} . If the free electron density is known, one can calculate all thermodynamic properties of the FG model. We get the chemical potential μ by numerical solution of $n_{fe}V = \int_0^\infty f(\epsilon)g(\epsilon)d\epsilon$, where V is the volume of space that constrains electron motion, $g(\epsilon) = 4\pi V(2m/\hbar^2)^{3/2}\epsilon^{1/2}$ is the FG density of states (DOS), m is the electron mass and h

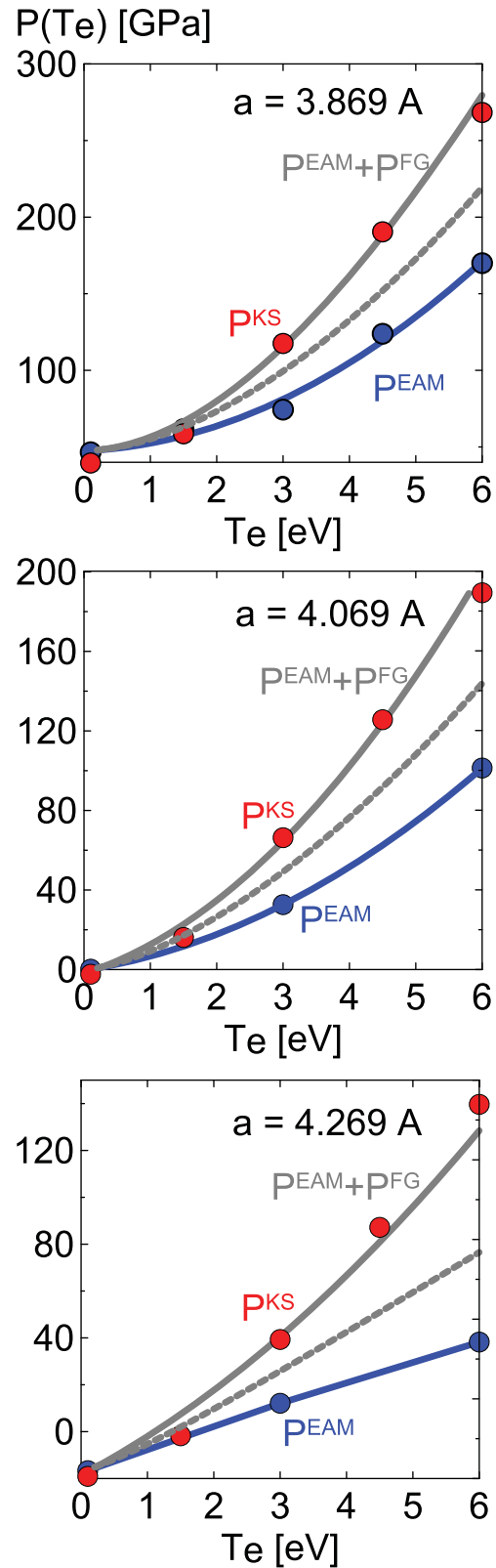


Figure 2. Comparison of pressure in the empirical classical interionic potential model (ETD EAM) P^{EAM} (the blue circles are the data and the blue line is an interpolation) and in the *ab initio* density functional theory model (FT KS DFT) P^{KS} (the red circles) obtained for fcc WDM gold at different densities (the lattice constants are shown). The sums of the EAM model pressure with the Fermi gas model pressure $P^{\text{EAM}} + P_{fe}^{\text{FG}}(n_{fe})$ are shown for $n_{fe} = 1$ electrons per atomic volume (dashed gray lines) and for $n_{fe} = 3$ electrons per atomic volume (solid gray lines).

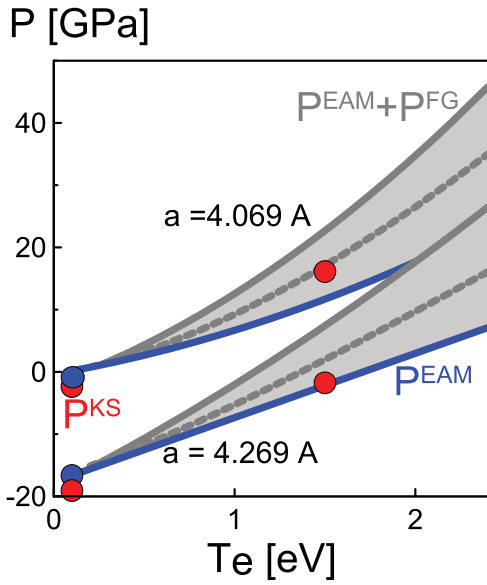


Figure 3. The same data as on Figure 2 for two values of the crystal lattice constant in the magnified scale. Grey filling is used to emphasise the data for a certain lattice constant.

is the Planck constant. Then, we get the internal energy $U = \int_0^\infty \epsilon f(\epsilon) g(\epsilon) d\epsilon$ and pressure $P_{fe}^{FG} = (2/3)U/V$.

Figure 2 suggests that

$$P^{KS} = P^{EAM} + P_{fe}^{FG}(n_{fe}; T_e). \quad (14)$$

The best fit of the pressure build-up by the sum $P^{EAM} + P_{fe}^{FG}$ gives $n_{fe} = 3 \pm 0.3$ electrons per atomic volume for the range $T_e = 1 - 6$ eV. The ETD EAM model [51–53] is based on three EAM potentials created for $T_e = 0.1, 3$ and 6 eV. Data for other T_e values are interpolated. That is why the accuracy of the $P^{EAM}(T_e)$ dependence at low T_e is currently not sufficient to determine the best n_{fe} at $T_e = 0 - 1$ eV by the $(P^{KS} - P^{EAM})$ fitting with P_{fe}^{FG} . It seems that $n_{fe} = 1$ electron could be a more accurate choice than three electrons. That could make sense since in this case the free electron number n_{fe} per one gold atom would change from the conventional value of 1 electron at $T_e = 0$ to 3 electrons at $T_e \gtrsim 1$ eV. The same data as on Figure 2 is presented on Figure 3 for two values of the lattice constant in the magnified scale in order to resolve low T_e points better (we omit $a = 3.869$ Å since the ETM EAM model performs not very well at high densities and low T_e).

Recent experimental data [83] suggest that 5d electrons have prominent contributions to the conduction electrons in WDM gold. These findings agree perfectly with our results if we assume that the electron temperature in [83] reaches $T_e \sim 1$ eV. In different experiments, different electron temperatures can be reached in 2T-WDM state resulting in different n_{fe} values.

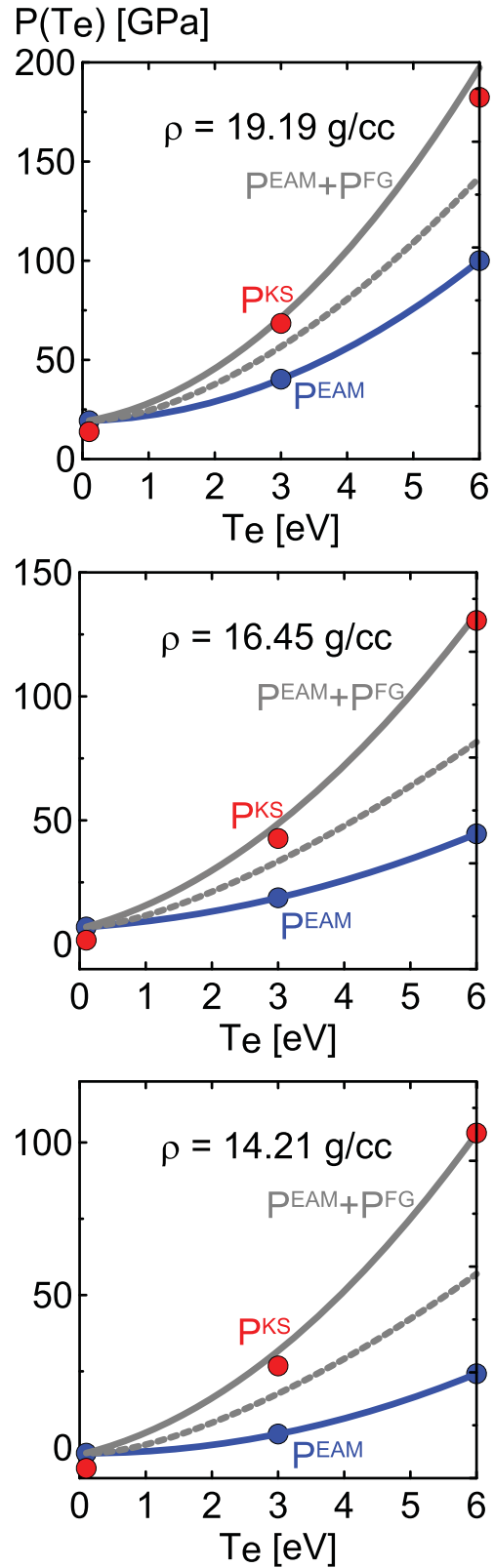


Figure 4. Comparison of pressure in the empirical classical interionic potential model (ETD EAM) P^{EAM} and in the *ab initio* density functional theory model (FT KS DFT) P^{KS} obtained for amorphous WDM gold at different densities (the values are shown). The sums the EAM model pressure with the Fermi gas model pressure $P^{EAM} + P_{fe}^{FG}$ are shown as on Figure 2 for $n_{fe} = 1$ and $n_{fe} = 3$.

Figure 2 shows that Equation (14) (with n_{fe} switching for 1–3 electrons per atomic volume) is valid for fcc WDM gold in a certain range of crystal densities.

In order to be sure that this result do not depend on the ionic structure, we make FT KS DFT calculations for amorphous WDM gold. Figure 4 shows the comparison of P^{EAM} and P^{KS} obtained for amorphous WDM gold at different densities. Again, we can see that Equation (14) holds and $n_{fe} = 3$ for $T_e > 1$ eV.

In the recent work of Bévilion and coauthors [84], a different approach for the calculation of n_{fe} has been used based on the fitting of the FT KS DFT electronic DOS by the square-root FG DOS. This approach gives $n_{fe} = 2.4 - 3.5$ electrons per ion for fcc Au for $T_e = 0 - 6$ eV. Their approach does not require the knowledge of the effective interionic potential. However, in [84] the authors did not see the correct asymptotic $n_{fe} \rightarrow 1$ as $T_e \rightarrow 0$.

7. Conclusions

The results presented in this work show that the FT KS DFT applied to WDM takes into account both bound and free electron states. There is no distinction between these state in the theory itself. However, we can introduce a certain criterium that can serve for their separation: the pressure build-up with increase of the electronic temperature T_e (for other variants see e.g. [85]). Here, we reveal this fact using an effective ion–ion potential obtained by FM. To our knowledge at the moment this is the only way for creation of such effective potentials for d-metals (the approach of [80] is developed for simple metals).

Using such effective potentials, we can estimate the ionisation degree (i.e. the number of free electrons per atoms) and its dependence in the electronic temperature T_e . As it was shown in [12] for simple metals like Al, there is no peculiarities (no deviation from the standard ‘valence’ of 3 electrons per atom). However, in the case of Au, we observe an interesting transition from 1 to 3 free electrons per atom at $T_e \sim 1$ eV. To our knowledge, there has been no theory that has predicted this ‘partial ionisation’ of d-electrons in WDM gold.

The connection (Equation (14)) between pressure in the *ab initio* FT KS DFT model and in the classical model with the effective ETD EAM potential brings us to the correspondence between (i) the ion–ion electrostatic energy together with the Kohn–Sham electronic free energy and (ii) the effective EAM ion–ion potential together with the FG free energy at the certain degree of ionisation

$$E_{ii}(\{\mathbf{R}_i\}) + \mathcal{F}_e^{KS}(\{\mathbf{R}_i\}; T_e) \leftrightarrow E_{ii}^{EAM}(\{\mathbf{R}_i\}; T_e) + \mathcal{F}_{fe}^{FG}(n_{fe}; T_e). \quad (15)$$

This relation can be treated as identity in the case of the equilibrium WDM with $T_i = T_e$. It can pave the way for the decoupled separate description of the dynamics of ion and electron subsystems in WDM. However, in the non-equilibrium case the applicability of ‘the quasi-equilibrium language’ for 2T-WDM is itself still an open question, moreover the effects of electron–ion energy transfer should be included in further studies.

Acknowledgments

We would like to thank Genri E. Norman for his guidance in the field of strongly coupled non-equilibrium Coulomb systems. V.V. Stegailov would like to thank Igor L. Iosilevskiy for stimulating discussions of free energy models. We gratefully acknowledge the access to the supercomputer K-100 of the Keldysh Institute of Applied Mathematics of RAS and to the supercomputer MVS-100 K of the Joint Supercomputer Center of RAS.


Disclosure statement

No potential conflict of interest was reported by the authors.

Funding

Russian Science Foundation [grant number 14-19-01487].

ORCID

V. V. Stegailov  <http://orcid.org/0000-0002-5349-3991>

References

- [1] R.J. Bartlett and M. Musiał, *Rev. Mod. Phys.* **79**, 291 (2007).
- [2] S. Hirata, *Mol. Phys.* **108** (21–23), 3113–3124 (2010).
- [3] J.J. Shepherd, T.M. Henderson, and G.E. Scuseria, *J. Chem. Phys.* **140**, 124102 (2014).
- [4] R. Dovesi, R. Orlando, A. Erba, C.M. Zicovich-Wilson, B. Civalieri, S. Casassa, L. Maschio, M. Ferrabone, M. De La Pierre, P. D’Arco, Y. Noel, M. Causa, M. Rerat, and B. Kirtman, *Int. J. Quantum Chem.* **114** (19), 1287–1317 (2014).
- [5] G.H. Booth, A. Grüneis, G. Kresse, and A. Alavi, *Nature* **493** (7432), 365–370 (2013).
- [6] F. Perrot and M.W.C. Dharma-wardana, *Phys. Rev. E* **52**, 5352 (1995).
- [7] P.L. Silvestrelli, A. Alavi, and M. Parrinello, *Phys. Rev. B* **55**, 15515 (1997).
- [8] M.P. Desjarlais, J.D. Kress, and L.A. Collins, *Phys. Rev. E* **66**, 025401 (2002).
- [9] V.V. Karasiev, S.B. Trickey, and F.E. Harris, *J. Comput.-Aided Mat. Des.* **13** (1–3), 111–129 (2006).
- [10] V.V. Karasiev and S.B. Trickey, *Comput. Phys. Commun.* **183** (12), 2519–2527 (2012).
- [11] J. Lehtomaki, I. Makkonen, M.A. Caro, A. Harju, and O. Lopez-Acevedo, *J. Chem. Phys.* **141**, 234102 (2014).
- [12] V. Stegailov and P. Zhilyaev, *Contributions Plasma Phys.* **55** (2–3), 164–171 (2015).

- [13] A.V. Bushman and V.E. Fortov, *Soviet Phys. Uspekhi* **26** (6), 465–496 (1983).
- [14] R. More, in *Advances in Atomic and Molecular Physics*, edited by D.R. Bates and Benjamin Bederson Elsevier Inc., Amsterdam, (1985), Vol. 21, pp. 305–356.
- [15] S. Glenzer, O. Landen, P. Neumayer, R. Lee, K. Widmann, S. Pollaine, R. Wallace, G. Gregori, A. Höll, T. Bornath, R. Thiele, V. Schwarz, W.D. Kraeft, and R. Redmer, *Phys. Rev. Lett.* **98**, 065002 (2007).
- [16] A.V. Lankin and G.E. Norman, *J. Phys. A: Math. Theoretical* **42**, 214032 (2009).
- [17] M.S. Murillo, J. Weisheit, S.B. Hansen, and M.W.C. Dharma-wardana, *Phys. Rev. E* **87**, 063113 (2013).
- [18] A. Ovechkin, P. Loboda, V. Novikov, A. Grushin, and A. Solomyannaya, *High Energy Density Physics* **13**, 20 (2014).
- [19] T. Ma, T. Döppner, R. Falcone, L. Fletcher, C. Fortmann, D. Gericke, O. Landen, H. Lee, A. Pak, J. Vorberger, K. Wünsch, and S. Glenzer, *Phys. Rev. Lett.* **110**, 065001 (2013).
- [20] H.R. Rüter and R. Redmer, *Phys. Rev. Lett.* **112**, 145007 (2014).
- [21] S. Vinko, O. Ciricosta, and J. Wark, *Nat. Commun.* **5**, 3533 (2014).
- [22] G.E. Norman, I.M. Saitov, and V.V. Stegailov, *Contrib. Plasma Phys.* **55** (23), 215–221 (2015).
- [23] B.Y. Mueller and B. Rethfeld, *Phys. Rev. B* **87**, 035139 (2013).
- [24] S. Gorbunov, P. Terekhin, N. Medvedev, and A. Volkov, *Nucl. Instrum. Methods Phys. Res. B* **315**, 173–178 (2013).
- [25] V.V. Pisarev and S.V. Starikov, *J. Phys. Condens. Matter* **26**, 475401 (2014).
- [26] V.K. Gryaznov and I.L. Iosilevskiy, *J. Phys. A Math. Theor.* **42**, 214007 (2009).
- [27] E. Liberatore, M.A. Morales, D.M. Ceperley, and C. Pierleoni, *Mol. Phys.* **109** (23–24), 3029–3036 (2011).
- [28] C. Vega, E. Sanz, J.L.F. Abascal, and E.G. Noya, *J. Phys. Condens. Matter* **20**, 153101 (2008).
- [29] D.E. Smirnova, S.V. Starikov, and V.V. Stegailov, *J. Phys. Condens. Matter* **24**, 015702 (2012).
- [30] T. Spura, C. John, S. Habershon, and T.D. Kuhne, *Mol. Phys.* **113** (8), 808–822 (2015).
- [31] A. Bratkovskii, V. Vaks, and A. Trefilov, *Sov. Phys. JETP* **59** (6), 1245–1255 (1984).
- [32] L.A. Falkovsky, *Physics-Uspekhi* **47** (3), 249–272 (2004).
- [33] E.G. Maksimov and A.E. Karakozov, *Physics-Uspekhi* **51** (6), 535–549 (2008).
- [34] S. Pisana, M. Lazzeri, C. Casiraghi, K.S. Novoselov, A.K. Geim, A.C. Ferrari, and F. Mauri, *Nat Mater* **6** (3), 198–201 (2007).
- [35] O. Shemyakin, P. Levashov, and K. Khishchenko, *Contrib. Plasma Phys.* **52** (1), 37–40 (2012).
- [36] N.D. Mermin, *Phys. Rev.* **137**, A1441 (1965).
- [37] J. Cao and B.J. Berne, *J. Chem. Phys.* **99** (4), 2902–2916 (1993).
- [38] M. French, T.R. Mattsson, N. Nettelmann, and R. Redmer, *Phys. Rev. B* **79**, 054107 (2009).
- [39] S. Root, R.J. Magyar, J.H. Carpenter, D.L. Hanson, and T.R. Mattsson, *Phys. Rev. Lett.* **105**, 085501 (2010).
- [40] K.H. Bennemann, *J. Phys. Condens. Matter* **16** (30), R995–R1056 (2004).
- [41] E. Gamaly, *Phys. Rep.* **508** (4-5), 91–243 (2011).
- [42] F.C. Kabeer, E.S. Zijlstra, and M.E. Garcia, *Phys. Rev. B* **89**, 100301 (2014).
- [43] G.E. Norman, I.Y. Skobelev, and V.V. Stegailov, *Contrib. Plasma Phys.* **51** (5), 411–418 (2011).
- [44] K. Sokolowski-Tinten, J. Bialkowski, A. Cavalleri, D. von der Linde, A. Oparin, J. Meyer-ter Vehn, and S.I. Anisimov, *Phys. Rev. Lett.* **81**, 224 (1998).
- [45] J. Chen, D. Tzou, and J. Beraun, *Int. J. Heat Mass Transf.* **49** (1-2), 307–316 (2006).
- [46] B. Chimier, V.T. Tikhonchuk, and L. Hallo, *Phys. Rev. B* **75**, 195124 (2007).
- [47] M.E. Povarnitsyn, T.E. Itina, K.V. Khishchenko, and P.R. Levashov, *Phys. Rev. Lett.* **103**, 195002 (2009).
- [48] M.E. Povarnitsyn, N.E. Andreev, P.R. Levashov, K.V. Khishchenko, and O.N. Rosmej, *Phys. Plasmas* (1994–present) **19**, 023110 (2012).
- [49] C. Schäfer, H.M. Urbassek, and L.V. Zhigilei, *Phys. Rev. B* **66**, 115404 (2002).
- [50] Y. Gan and J.K. Chen, *Appl. Phys. Lett.* **94** (20), 201116 (2009).
- [51] S. Starikov, V. Stegailov, G. Norman, V. Fortov, M. Ishino, M. Tanaka, N. Hasegawa, M. Nishikino, T. Ohba, T. Kaihori, E. Ochi, T. Imazono, T. Kavachi, S. Tamotsu, T. Pikuz, I. Skobelev, and A. Faenov, *JETP Lett.* **93** (11), 642–647 (2011).
- [52] G. Norman, S. Starikov, and V. Stegailov, *J. Exp. Theor. Phys.* **114** (5), 792–800 (2012).
- [53] G. Norman, S. Starikov, V. Stegailov, V. Fortov, I. Skobelev, T. Pikuz, A. Faenov, S. Tamotsu, Y. Kato, M. Ishino, M. Tanaka, N. Hasegawa, M. Nishikino, T. Ohba, T. Kaihori, Y. Ochi, T. Imazono, Y. Fukuda, M. Kando, and T. Kawachi, *J. Appl. Phys.* **112**, 013104 (2012).
- [54] S.L. Daraszewicz, Y. Giret, N. Naruse, Y. Murooka, J. Yang, D.M. Duffy, A.L. Shluger, and K. Tanimura, *Phys. Rev. B* **88**, 184101 (2013).
- [55] Y. Rosandi and H. Urbassek, *Appl. Phys. A* **110** (3), 649–654 (2013).
- [56] N.A. Inogamov, V.V. Zhakhovskiy, Y.V. Petrov, V. Khokhlov, S.I. Ashitkov, K.V. Khishchenko, K.P. Migdal, D.K. Ilnitsky, Y.N. Emirov, P.S. Komarov, V.V. Shepelev, C. Miller, I. Oleynik, M. Agranat, A. Andriyash, S. Anisimov, and V. Fortov, *Contrib. Plasma Phys.* **53** (10), 796–810 (2013).
- [57] C. Wu and L.V. Zhigilei, *Appl. Phys. A* **114** (1), 11–32 (2014).
- [58] Y. Shen, Y. Gan, W. Qi, Y. Shen, and Z. Chen, *Appl. Opt.* **54** (7), 1737–1742 (2015).
- [59] S.V. Starikov and V.V. Pisarev, *J. Appl. Phys.* **117**, 135901 (2015).
- [60] L. Falkovsky and E. Mishchenko, *J. Exp. Theor. Phys.* **88** (1), 84–88 (1999).
- [61] G. Kresse and J. Hafner, *Phys. Rev. B* **47**, 558 (1993).
- [62] G. Kresse and J. Hafner, *Phys. Rev. B* **49**, 14251 (1994).
- [63] G. Kresse and J. Furthmüller, *Comput. Mat. Sci.* **6** (1), 15–50 (1996).
- [64] G. Kresse and J. Furthmüller, *Phys. Rev. B* **54**, 11169 (1996).
- [65] P.E. Blöchl, *Phys. Rev. B* **50**, 17953 (1994).
- [66] G. Kresse and D. Joubert, *Phys. Rev. B* **59**, 1758 (1999).

- [67] J. Perdew and A. Zunger, *Phys. Rev. B* **23**, 5048 (1981).
- [68] V. Recoules, J. Clérouin, G. Zérah, P.M. Anglade, and S. Mazevet, *Phys. Rev. Lett.* **96**, 055503 (2006).
- [69] R. Ernstorfer, M. Harb, C.T. Hebeisen, G. Sciaini, T. Dartigalongue, and R.J.D. Miller, *Science* **323** (5917), 1033–1037 (2009).
- [70] V. Stegailov, *Contrib. Plasma Phys.* **50** (1), 31–34 (2010).
- [71] E. Zijlstra, A. Kalitsov, T. Zier, and M. Garcia, *Phys. Rev. X* **3**, 011005 (2013).
- [72] M. Weinert and J.W. Davenport, *Phys. Rev. B* **45**, 13709 (1992).
- [73] N.L. Doltsinis and D. Marx, *J. Theor. Comput. Chem.* **01** (02), 319–349 (2002).
- [74] N. Medvedev, V. Tkachenko, and B. Ziaja, *Contrib. Plasma Phys.* **55** (1), 12–34 (2015).
- [75] N. Medvedev, Z. Li, and B. Ziaja, *Phys. Rev. B* **91**, 054113 (2015).
- [76] S. Khakshouri, D. Alfè, and D.M. Duffy, *Phys. Rev. B* **78**, 224304 (2008).
- [77] S.M. Foiles and M.I. Baskes, *MRS Bulletin* **37**, 485 (2012).
- [78] S. Plimpton, *J. Comput. Phys.* **117** (1), 1–19 (1995).
- [79] S.J. Plimpton and A.P. Thompson, *MRS Bull.* **37**, 513 (2012).
- [80] L. Harbour, M.W.C. Dharma-wardana, D.D. Klug, and L.J. Lewis, *Contrib. Plasma Phys.* **55** (2–3), 144–151 (2015).
- [81] J.A. Zimmerman, E.B. Webb III, J.J. Hoyt, R.E. Jones, P.A. Klein, and D.J. Bammann, *Modelling Simul. Mat. Sci. Eng.* **12** (4), S319–S332 (2004).
- [82] R. Bystryi, Y. Lavrinenko, A. Lankin, I. Morozov, G. Norman, and I. Saitov, *High Temp.* **52** (4), 475–482 (2014).
- [83] A. Sekiyama, J. Yamaguchi, A. Higashiya, M. Obara, H. Sugiyama, M.Y. Kimura, S. Suga, S. Imada, I.A. Nekrasov, M. Yabashi, K. Tamasaku, and T. Ishikawa, *New J. Phys.* **12**, 043045 (2010).
- [84] E. Bévilion, J.P. Colombier, V. Recoules, and R. Stoian, *Phys. Rev. B* **89**, 115117 (2014).
- [85] G. Norman, I. Saitov, V. Stegailov, and P. Zhilyaev, *Phys. Rev. E* **91**, 023105 (2015).